atmosphere

Article

Heatwaves and Their Impact on Air Quality in Greater Cairo, Egypt

Amira N. Mostafa [1,2,*], Stéphane C. Alfaro [3], Sayed. M. Robaa [2], Ashraf S. Zakey [1] and Mohamed M. Abdel Wahab [2]

[1] Egyptian Meteorological Authority, Cairo P.O. Box 11784, Egypt; ashzakey@gmail.com
[2] Astronomy, Space Science and Meteorology Department, Faculty of Science, Cairo University, Giza P.O. Box 12613, Egypt; robaa@sci.cu.edu.eg (S.M.R.); magdy@sci.cu.edu.eg (M.M.A.W.)
[3] Université de Paris Est Créteil and Université de Paris, CNRS, LISA, F-94010 Créteil, France; stephane.alfaro@lisa.ipsl.fr
* Correspondence: amira_nasser@pg.cu.edu.eg; Tel.: +20-10-0767-6001

Abstract: Several heatwaves (HWs) have been recorded in Egypt in recent years. Some of these HWs were mild, while others were severe and resulted in mortalities and morbidities. On the other hand, air pollution is considered a health issue in Egypt's megacities, especially the capital city, Cairo, and its surroundings, the Greater Cairo (GC) region. In this study, we examine a number of HWs that have hit Egypt in recent years, along with the state of air quality, in terms of PM10, NO_2, and O_3, during the period of HW incidence, with a focus on the GC region. During the period of study, the frequency, intensity, and duration of HWs have been observed to increase. The total number of recorded HW events was 190, encompassing 376 HW days. The time series of daily mean NO_2 showed no correlation with temperature during the months that experienced HWs cases. Conversely, PM10 and O_3 concentrations exhibited a similar pattern as that of the daily maximum temperature. This increase in the two pollutant concentrations led to a degradation of the air quality, as demonstrated by the fact that the Air Quality Health Index went from "moderate risk", on normal days, to "high risk" during the HWs.

Keywords: extreme weather events; air pollution; particulate matter; nitrogen dioxide; ozone; air quality health index; risk assessment; megacities

check for updates

Citation: Mostafa, A.N.; Alfaro, S.C.; Robaa, S.M.; Zakey, A.S.; Abdel Wahab, M.M. Heatwaves and Their Impact on Air Quality in Greater Cairo, Egypt. *Atmosphere* **2024**, *15*, 637. https://doi.org/10.3390/atmos15060637

Academic Editor: Michael L. Kaplan

Received: 26 April 2024
Revised: 22 May 2024
Accepted: 24 May 2024
Published: 25 May 2024

1. Introduction

Heatwaves (HWs) are caused by very hot, stagnant air masses. They form when high pressure aloft (3000–7600 m) strengthens and remains over a region for several days up to several weeks, while dew points are high and wind speeds are often low. Moreover, clear or partly cloudy skies allow intense solar energy to further heat the ground and the air mass. This situation is common in summer, as summertime weather patterns are generally slower to change than those in winter, which results in slower movement of this upper-level high pressure system [1].

There is no formal, standardized definition of a heatwave (HW). An HW can be defined as "a period of abnormally hot weather generally lasting more than two days" [2] or can be defined as "an extended period of hot weather relative to the expected conditions of the area at that time of year, which may be accompanied by high humidity" [1]. Also, HW is defined according to the Glossary of Meteorology as "a period of abnormally and uncomfortably hot and usually humid weather" [3]. Normally, an HW is measured relative to the usual weather in a certain area and relative to normal temperatures for the season [4]. According to the World Meteorological Organization (WMO) and Frich et al.'s HW Duration Index [5], an HW occurs when the daily maximum temperature of more than five consecutive days exceeds the average maximum temperature by 5 °C (9 °F), the normal reference period being the years from 1961–1990; however, recently, the WMO defined the HW as "a marked

unusual period of hot weather over a region persisting for at least two consecutive days during the hot period of the year based on local climatological conditions, with thermal conditions recorded above given thresholds" [6].

Severe HWs can cause several adverse consequences, such as health, psychological, sociological, and economic effects. They cause catastrophic crop failures and thousands of deaths from hyperthermia, which is also known as heat stroke. High humidity and elevated nighttime temperatures appear to be key factors in causing heat-related illness and mortality. Heat stress occurs in humans when the body is unable to cool itself effectively. Normally, the body can cool itself through perspiration, or sweating. However, high relative humidity reduces the evaporation rate. This results in a lower rate of heat removal from the body, hence the sensation of being overheated, potentially leading to heat stroke. When there is no break from the heat at night, it can cause discomfort and lead to health problems, especially for the poor, young, and elderly. Therefore, lives are endangered when these conditions persist all day long for several days. Extremely warm weather exacerbates the negative health effects of both heat and air pollution, and the deteriorated air quality status may increase the mortality and morbidity toll of an extreme heat event. This can worsen chronic respiratory and cardiovascular conditions, as well as cause heat exhaustion, cramps, heat stroke, and in certain cases, heat-related mortality. Those with chronic conditions, the elderly, women, and children are among the most vulnerable groups [7,8].

According to a World Bank report [9], the death toll of the 2003 HW in France was estimated at 70,000 and that of the 2010 HW in Russia was estimated at 55,000, with more than 1 million hectares of burned land. The WMO announced that the severe HWs of 2003 and 2010 accounted for 80% of weather-related deaths in Europe from 1970–2019 [10].

In a study shedding light on whether the global research is proportional to the growing threat of HWs, Klingelhöfer et al. [11] reported that the exposure of the populations to HWs in some countries, including Egypt, is rising sharply, while the body of research on HWs does not reflect this threat. However, there exists some scientific research which include studies on the HWs over Egypt and their relationship with human comfort and health, as well as other areas.

Aboelkhair and Morsy [12] studied the extreme warm and cold events over Egypt between 1981 and 2020. They showed that the daily maximum and daily minimum temperatures increased gradually throughout the study period, with south Egypt exhibiting the highest daily minimum temperature values.

Morsy and El Afandi [13] used the ClimPACTv2 software to identify the decadal changes in the HWs indices over Egypt during the period from 1979 to 2018. The results revealed that the decadal summations of the HW number, duration, and frequency increased significantly in the last decade (2009–2018), with the southeastern part of Egypt subjected to a higher summation of HW amplitude and HW magnitude than the northwestern part, especially during the last two decades.

In a study on the extreme temperature events over Egypt, Saleh et al. [14] investigated the HW cases during the period from 1980 to 2015 in three governorates in Egypt, with a focus on the major agricultural climatic regions, namely Behira governorate, representing North Delta; Giza governorate, representing Middle Egypt; and Qena governorate, representing Upper Egypt. This study found that Egypt was exposed to several HW events during the last decades, the most pronounced being the HWs of the winter season of 2010 and the summer season of 2015. It was also found that the highest monthly maximum air temperature recorded in the summer season for El-Behira was in August 2015, with a temperature of 33.4 °C, followed by August 2012, while the highest severe HWs were recorded in the winter season of 2010, with a temperature of 22.6 °C. In addition, the highest reduction of productivity for wheat and maize, which are major cereal crops in Egypt, was recorded in Upper Egypt, followed by Middle Egypt, while the lowest reduction was recorded in North Delta for wheat (winter season) and maize (summer season).

Ceccherini et al. [15] studied the HWs across Africa over recent years (1981–2015) and stated that the major hot spot for the increases in HW frequency and magnitude in Africa included Egypt and the whole northern Africa region.

Regarding the air pollution state of the Greater Cairo (GC) region, a study by Mostafa et al. [16] for the period between 2010–2014 over GC revealed that the hourly averaged concentrations of sulfur dioxide (SO_2), nitrogen dioxide (NO_2), carbon monoxide (CO), ozone (O_3), and particulate matter measuring 10 μm or less in diameter (PM10) in some parts of GC were as high as 29.1 $\mu g/m^3$, 61.1 $\mu g/m^3$, 8.5 $\mu g/m^3$, 21.3 $\mu g/m^3$, and 223.2 $\mu g/m^3$, respectively. The almost half-yearly average (May–December) of PM2.5 in 2022 was 125.6 $\mu g/m^3$, according to the AirNow Department of State, Cairo US Embassy Air Quality project [17].

Recent works suggest that HWs could have a direct impact on the concentration of some air pollutants, thus aggravating their adverse health effects. Theoharatos et al. [18] investigated the relationship between the HWs of 2007 and air pollution levels in Athens, Greece. Poor air quality conditions were observed for the HW of July, with a significant correlation found between the heat load index and average hourly concentrations of NO_2, SO_2, and O_3, while in the June HW, there was an increased number of reported heat-affected patients. In their study focused on Manchester, Kalisa et al. [19] examined the correlation between temperature and air pollution during the months that experienced HW cases and stated that the emission of air pollutants may be aggravated during HWs, and this may result in the negative impact of high temperatures on sensitive groups, leading to increased mortality levels. Khomsi et al. [20] investigated the concurrency of HWs and extreme O_3 episodes in two cities in Morocco—Casablanca and Marrakech—while examining the atmospheric conditions that may lead to their occurrence. They found that the concurrency of HWs and O_3 depends on geographical and local characteristics of the city and large-scale atmospheric circulation, stating that this finding would pave the way for the establishment of a warning system for such hazards.

On the other hand, Pascal et al. [21] debated the need for a joint public health warning for HWs and acute air pollution episodes. In their work, they examined the effect of seasonality and temperature on air pollution (PM10 and O_3)-related mortality on one hand, and the impact of air pollution on heat-related mortality on the other hand. They found that air pollution-related mortality varied among spring, summer, and HWs, and that there was a high influence of air pollution on heat-related mortality, especially during the most severe HWs. They recommended taking seasonality and HWs into account when issuing air pollution warnings, while they concluded that there is a limited value added from including air pollution information into the HW warning systems, compared to the increased complexity it would impose to the warning systems.

This study aims at investigating some of the most pronounced HWs that have hit Egypt in past years, along with examining the air quality state, in terms of PM10, NO_2, and O_3 concentrations, during the period, with a focus on the GC region. Special attention will be paid to the quantification of the potential correlation between extreme heat events and episodes of high air pollution.

2. Materials and Methods

2.1. Study Area

Mostafa et al. [22] analyzed the past and future temperature and precipitation trends at eight locations representative of the variety of Egyptian climates and found that despite the fact that these eight locations are quite distant from each other, their year-to-year patterns of temperature and precipitation were the same. This shows that the HWs are large-scale phenomena striking all of Egypt simultaneously.

The GC is the name given to the metropolitan region, which spans three governorates (Cairo, Giza, and Qalyubia) and covers a total area of 2670 km^2. According to the last national census, the GC's estimated population is as high as 26.02 million, with a population

density of around 9743.8 people/km^2. In this densely populated megacity, air pollution is a serious environmental problem that affects both the urban and rural areas [23].

2.2. Temperature Data

The meteorological dataset comprised hourly temperature data, measured by the Egyptian Meteorological Authority (EMA) at the Cairo Airport station. The available dataset was recorded during the period of January 2005 until October 2023. The daily maximum and average temperature values were calculated from this dataset. Also, a daily maximum temperature dataset for a reference period of 1982–2010 was available for the Cairo Airport station.

2.3. Air Quality Data

The air quality dataset comprised daily concentrations of PM10, NO_2, and O_3 measured by the Egyptian Environmental Affairs Agency (EEAA) for the El-Abbasseya station (a station not far from Cairo Airport station, around 17 km away). The air pollution concentrations are measured continuously, on an hourly basis. The quality of the measurements has been discussed in previous papers, e.g., Refs. [16,23–26]. In this study, the available EEAA dataset was gathered for the period from 2005 until 2018 as daily averages, with some gaps in 2010 and 2012. In an attempt to compensate for these gaps, the PM10 and O_3 measurements performed by the EMA for El-Abbasseya in 2010 (PM10), as well as in 2010 and 2012 (O_3), were also used.

2.4. Methodology

2.4.1. Heatwave Definition

Several experiments were conducted to determine the most appropriate methodology to identify the HWs. The approach of identifying HWs based on thresholds relative to historical temperature distributions (e.g., the 90th or 95th percentile) was tested. However, the 90th percentile of the maximum and minimum temperature values for the available reference period of 1982–2010 were calculated to be 36.7 °C and 22 °C (average temperature of 29.4 °C), respectively, which seemed to exaggerate the results of identifying the HW events and days, and the 95th percentile for maximum and minimum temperature values for the available reference period were calculated to be 37.9 °C and 22.8 °C (average temperature of 30.4 °C), respectively, which seemed to show a lower effectiveness in capturing days with anomalously high temperatures. Additionally, both percentiles underrated the HW of 2023, which had pronounced adverse effects on the energy and health sectors.

On the other hand, as it was observed to be most convenient for Egypt's climate, in this study, we adopted the HW definition proposed by Metaxas and Kallos [27]. Namely, an HW day is defined based on two temperature criteria, as follows: the daily maximum and the daily average temperature value should be at least 37 °C and 31 °C, respectively [28]. Despite the fact that Egypt has a common occurrence of a maximum temperature of 37 °C, the presence of another condition, i.e., an average temperature of at least 31 °C, made this approach more effective in capturing days with anomalously high temperatures and in characterizing the occurrence of HW events that resulted in adverse health outcomes and negative impacts on multiple sectors, such as the energy sector.

2.4.2. Data Analysis

The characteristics of the recent HWs were determined based on the following:

1. Analysis of the HW intensity, in terms of the number of HW days and the maximum temperature reached during an HW event;
2. Analysis of the HW frequency, in terms of the number of HW events.

The relationship between daily mean temperature and air pollution levels, in terms of PM10, NO_2, and O_3 concentration, during HW periods for GC was assessed based on the following:

1. Analysis of the time series of daily mean temperature and air pollutant concentration during the months that recorded severe HW events [19].
2. Analysis of correlation between the temperature and each of the air pollutants, using a simple linear regression model (linear correlation model) [19].
3. Analysis of the Air Quality Health Index (AQHI), which measures the air quality in relation to public health, taking into account the daily averaged concentrations of PM10, NO_2, and O_3 on a scale of 1 to 10. The largest AQHI corresponds to the highest health risk from air pollution. The AQHI [29] also provides a word classification that describes the degree of health risk related to the index reading (such as Low, Moderate, High, or Very High Health Risk). It is calculated according to Equation (1) [23,30]. Table 1 shows the health risk as class indices, along with the AQHI grid showing associated health messages:

Table 1. AQHI grid corresponding to each health risk class index [29].

Health Risk Index Class	AQHI Grid
Low Risk	1–3
Moderate Risk	4–6
High Risk	7–10
Very High Risk	10+

$$\text{AQHI} = \left(\frac{10}{10.7}\right) \times 100 \times \left[\left(e^{0.000297 \times PM_{10}} - 1\right) + \left(e^{0.000871 \times NO_2} - 1\right) + \left(e^{0.000537 \times O_3} - 1\right)\right] \quad (1)$$

3. Results

3.1. Characteristics of Recent HWs

The number of HW events and the number of HW days that were identified per year during the period of January 2005 until October 2023 are illustrated in Figure 1. Based on the HW definitions applied in this study [27], the total number of recorded HW events was 190 cases, with 376 HW days. During the whole period of study, there was not a single year that did not record an HW. The highest annual number of HW events was observed in the year 2008, when 16 HW events were detected, followed by 2010 and 2016, which recorded 15 HW events. On the other hand, the year 2021 recorded the highest number of HW days (44 days), followed by 2010 (30 days), and 2016 (29 days). The slope of the linear fit (black dashed line in Figure 1) is positive, which means that the number of yearly HW days increased over the period of study.

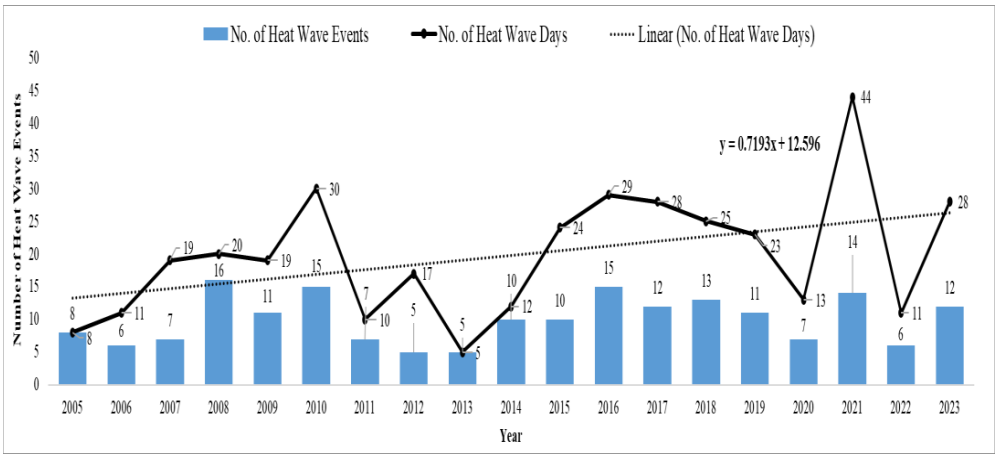

Figure 1. Number of identified HW events (blue bars) and HW days (solid black curve with black circles) during the period 2005–2023. Black dashed line: linear fit.

In 2005 and 2013, all the HWs lasted only one day (1-day HW), whereas HWs of two or more consecutive days were recorded in the other years. It was also clearly observed that the frequency of HW events lasting at least two consecutive days increased markedly after the year 2015.

The daily maximum temperature values that were recorded during the identified HW days are plotted in Figure 2. During the period of study, it is shown that peak temperatures higher than 41 °C were observed, starting from the year 2006. Similarly, the average and maximum durations of the HW events observed each year tended to increase (*p*-values of 0.32 and 0.13, respectively) (Figure 3). The first long (i.e., with a duration of at least 3 days) HW event was observed in 2006 and lasted 5 days. The most prolonged event was observed in 2021, when 11 consecutive days were identified as HW days. Interestingly, the hottest HW events are not necessarily the longest: for instance, in 2013, all five HW events lasted just one day, but their temperatures exceeded 41 °C. However, the results show that over the period of study, there is a general increase in the frequency of occurrence of the HWs, as well as an increase in their duration; however, longer observational time series would be necessary to confirm these result.

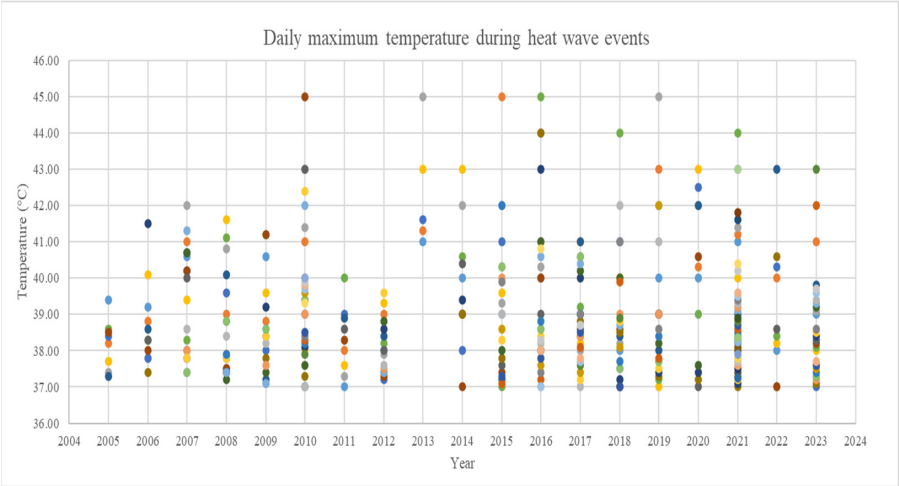

Figure 2. Maximum temperature of the observed HW days during the period of January 2005 until October 2023. The colors indicate different HWs cases each year.

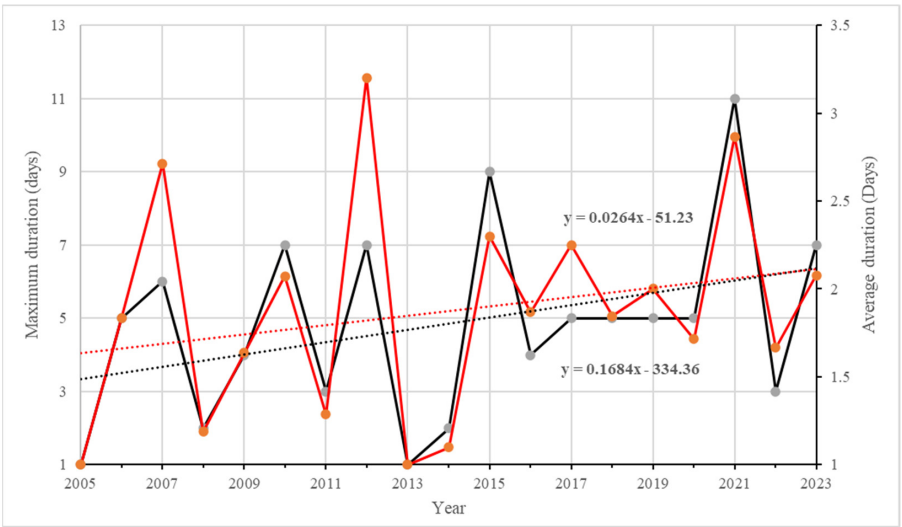

Figure 3. Evolution of the average (red curve) and maximum (black curve) durations of the heat events recorded in GC each year between 2005 and 2023. The dotted lines are the best linear fits of the two plots.

HWs not only occurred during summer seasons (June–August), but also in March, April, May, September, and October. However, the frequency of their occurrence in summer is much larger. Figure 4 shows that over the last 18 years, most of the years witnessed the occurrence of HW days between May and September, except for the years 2008, 2011, 2016, 2021, and 2022, in which HW days occurred earlier (in March for 2008 and April for the rest of those years), and for the year 2009 and 2020, which ended in October. This indicated that those mentioned years had longer periods prone to HW occurrence.

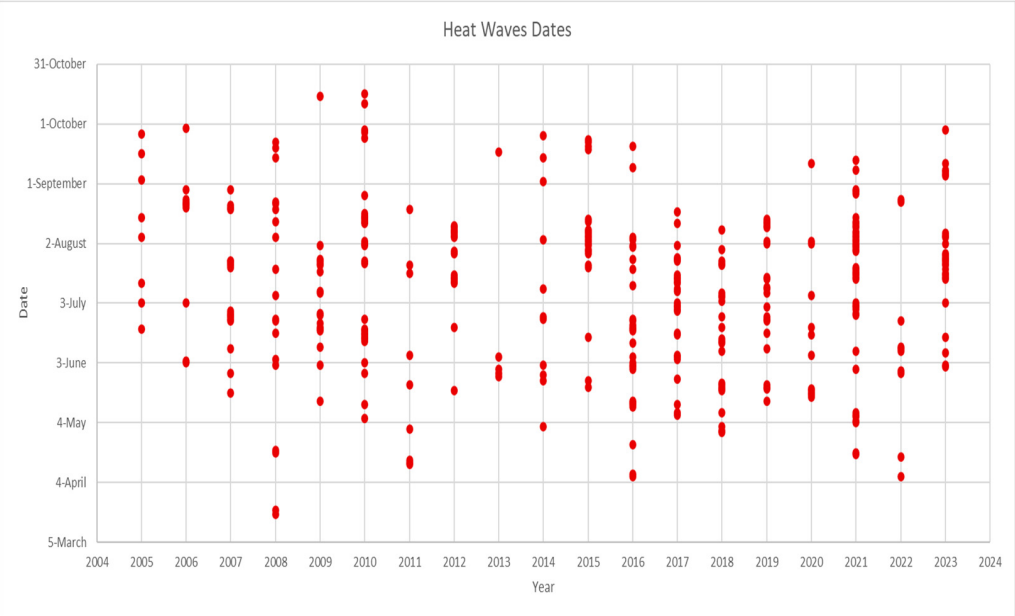

Figure 4. Dates during the period between 2005 and 2023 when the HW days occurred.

3.2. Assessment of the Relationship between Temperature and the Pollutant Concentrations during HWs

3.2.1. Selection of the Periods of Study

Because the longest HWs are expected to have the largest potential effect on air quality, the rest of this study is focused only on the severe HWs. Therefore, in the first stage, only the years with consecutive HWs days were retained; then, in these years, the month(s) with the maximum number of HW days were selected. Finally, to narrow down the selection, a criterion was used to further filter the HWs: only those with a duration above the general average (5 days) were considered. As a result of this process, the most severe HWs were found to have occurred in 2007, 2010, 2012, 2015, 2021, and 2023. Table 2 reports the exact dates of these HWs, their duration (N, in days), the fraction (%) of the total number of HW days in the year contributed by these specific HWs, and other useful indicators, such as the average maximum temperature (Tmax) and the average concentrations of PM10, NO_2, and O_3. Note that the latter concentrations were not always available.

3.2.2. Time Series Analysis of Temperature and PM10 Concentration during Months with Severe HWs

In order to examine the correlation between the temperature and the PM10 concentration, time series of daily maximum temperature and daily mean concentration of air pollutants were plotted for the months shown in Table 2 that had concentration data (Figure 5). In 2007 and 2010, there is a clear tendency for the concentration to increase with the temperature ($p \leq 0.05$). In 2012, there was also a positive correlation, but the fact that the PM10 concentration remained relatively moderate for GC (around 50 $\mu g/m^3$) masks, in large part, its variations. Conversely, in 2015, an isolated huge peak of PM10 (at 1288 $\mu g/m^3$) occurred on 3 August due to the advection of mineral dust from the deserts surrounding GC. Had it been represented on the plot, it would have made it impossible to

observe the positive correlation linking the PM10 concentration to Tmax. This correlation is particularly clear during the first 22 days of July.

Table 2. Details of the most severe HW periods identified between 2005 and 2023 in the GC area (see selection criteria in the text). For the concentrations, Nil corresponds to missing data.

Year	Month	Period	N (%)	Tmax (°C)	PM10 (μg/m^3)	NO_2 (μg/m^3)	O_3 (μg/m^3)
2007	June	24–29th	6 (31.6)	39.8	134.1	Nil	Nil
	July	24–28th	5 (26.3)	39.2	146.2	Nil	Nil
2010	June	17–23rd	7 (23.3)	39.9	186.0	14.7	13.1
	August	15–20th	6 (20.0)	38.3	108.7	16.2	12.5
2012	August	7–13th	7 (41.2)	37.6	49.4	22.9	39.6
2015	August	3–11th	9 (37.5)	38.3	312.1	18.8	37.0
2021	July	15–21st	7 (15.9)	38.0	Nil	Nil	Nil
	July–August	29–8th	11 (25.0)	39.9	Nil	Nil	Nil
2023	July	22–28th	7 (25.0)	38.4	Nil	Nil	Nil

3.2.3. Correlation Analysis of Temperature and Air Pollution

More quantitatively, the dependence of the PM10 concentration on Tmax can be evaluated by calculating the average PM10 and its standard deviation in each temperature bin comprising a span of 1 °C between 27.5 and 40.5 °C. Note that in the calculation of the averages, the extremely large PM10 values (i.e., those above 220 μg/m^3, which is the 95th percentile of the statistical distribution) that are due to the advection of mineral dust from the deserts surrounding GC were considered as outliers and were not taken into account. The very large value of the coefficient of determination (R^2 = 0.84) confirms the strength of the influence of Tmax on PM10, and the slope of the linear best fit to the results (Figure 6) indicates that for each 1 °C increase in Tmax, the average increase in PM10 is 4.7 μg/m^3. Over the range of temperature considered in our study, this corresponds to a quasi-doubling of the PM10 concentration (Figure 6).

For NO_2 and ozone, the visual examination of the time series (not shown) does not reveal any obvious covariation with the temperature. However, the methodology previously used for PM10 was also applied to these two pollutants. This method confirms the absence of the influence of Tmax on the concentrations of NO_2 (R^2 = 0.001, Figure 7a). During the months exhibiting the severe HWs, the average daily NO_2 concentration varied around 31 (±12) μg/m^3, independently of the temperature. Regarding ozone (Figure 7b), there is a significant positive correlation (R^2 = 0.24) with the temperature, but the slope is so modest that the average increase in the O_3 concentration is only 5.9 μg/m^3 between 30 and 40 °C. This increase represents about 10% of the average concentration (58 ± 6 μg/m^3) of the period of study and is much smaller than the quasi doubling of the PM10 for the same range of temperature variations.

3.2.4. Implications for AQHI during HWs

In Equation (1), the numerical evaluation of the three terms of the summation allows for separately quantifying the effects of PM10, NO_2, and O_3 on the overall AQHI. Our results show that during the summer months, NO_2 is little affected by the occurrence of the HWs, which means that its contribution to the AQHI is relatively constant. With an average concentration of 31 μg/m^3 (see above and Figure 7a), this contribution is 2.6 (CI, 1.6–3.6), which—were NO_2 considered alone—would correspond to a low risk (Table 1). When the temperature increases from about 30 to 40 °C (the latter value being representative of intense HWs), the average concentration of ozone increases from 52 to 64 μg/m^3, that of PM10 from 60 to 120 μg/m^3, and their individual contributions to the AQHI from 2.6 to 3.3 (ozone), and from 1.7 to 3.4 (PM10). In summary, the average AQHI is 6.9 at 30 °C, but it

reaches 9.3 at 40 °C. This increase is mostly due to the contribution of PM10, and the health risk shifts from "moderate" to "high" (Table 1).

Therefore, with an increasing frequency of HW days (Figure 1), one can expect a degradation of the general air quality in GC, particularly in the summer months. This impact is further illustrated by Figure 8, showing the good correlation (R^2 = 0.56) between the number of yearly HW days between 2009 and 2016 and the average AQHI in the same period.

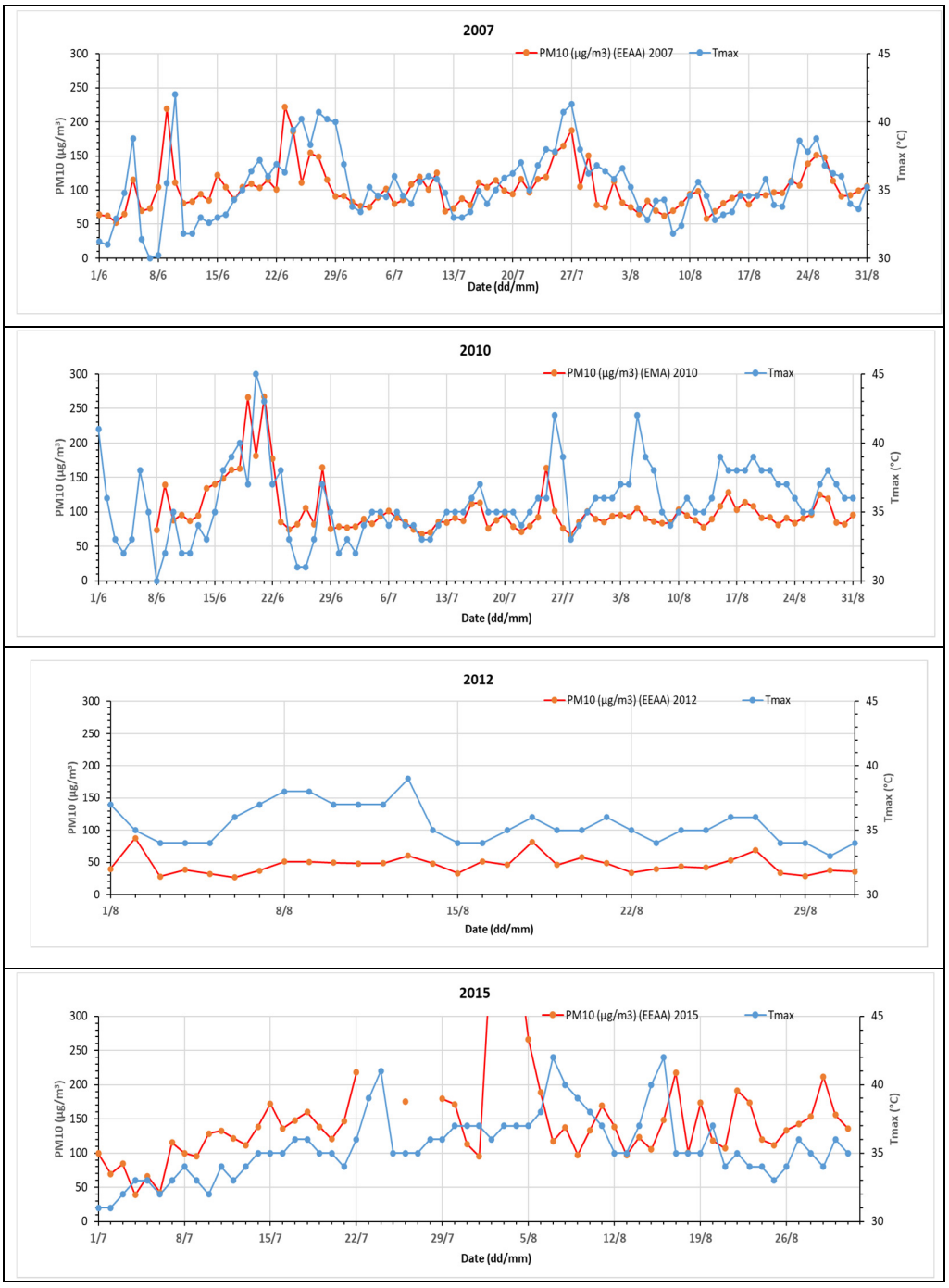

Figure 5. Co-variations of the daily Tmax and the PM10 concentrations during the summer months of the severe HWs reported in Table 2.

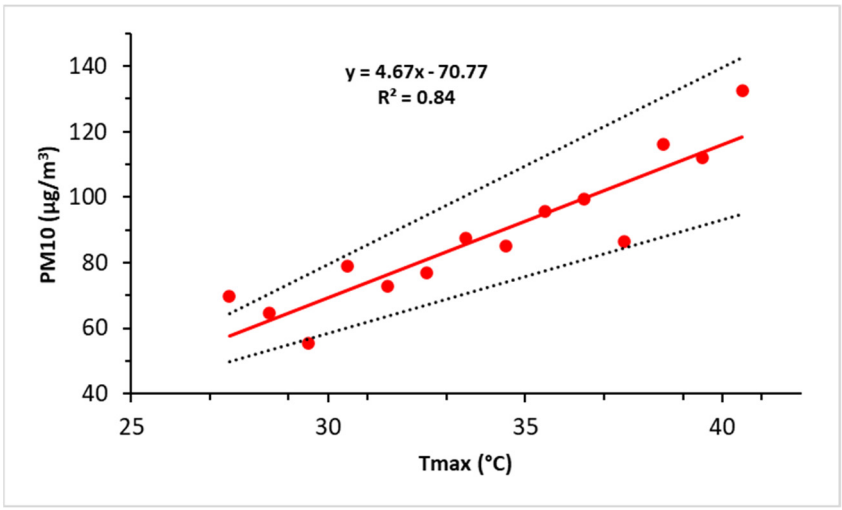

Figure 6. Influence of the increase in temperature on the average PM10 concentration in the GC area (red points). The red line is the best fit to the observations, and the distance between the dotted lines corresponds to one standard deviation.

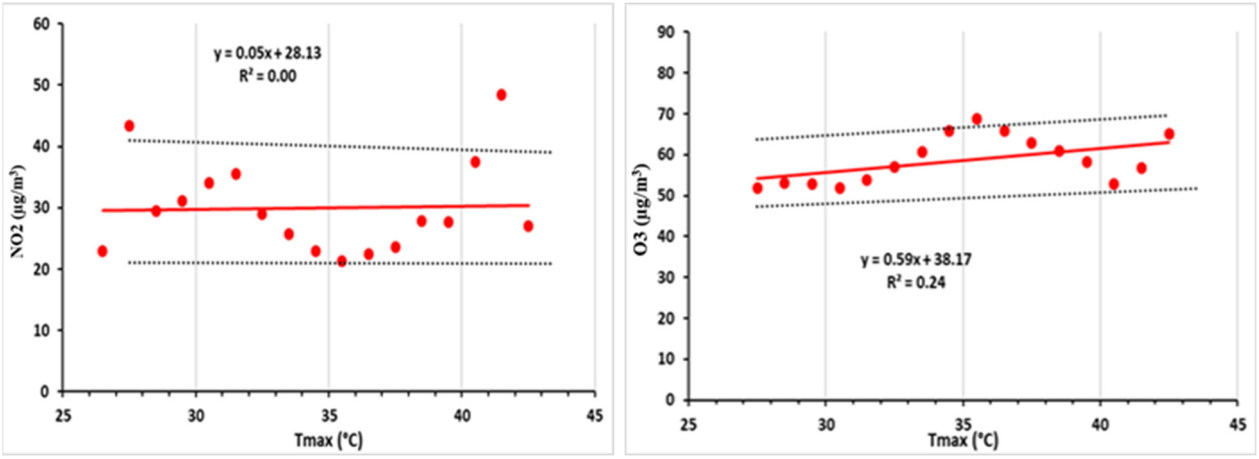

(**a**) (**b**)

Figure 7. Same as Figure 6, but for (**a**) NO_2 and (**b**) O_3.

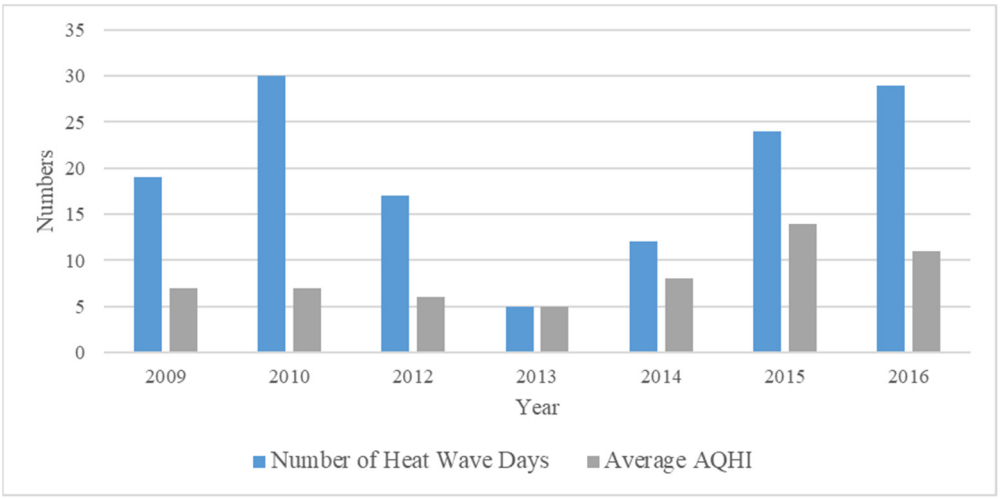

Figure 8. Number of HW days of each year versus the average AQHI for the same years.

4. Discussion

Interestingly, summer is not a season during which the advection of desert dust (frequent in spring) or biomass burning (September and October) is usually observed. This means that we have mostly looked at the effect of temperature on the concentration of PM10, NO_2, and ozone produced locally.

There is not a lot of literature examining the correlation between HWs and air quality in Egypt. One study conducted by Mohamed et al. [31] regarding the interaction between air pollution and thermal discomfort, which considers temperature and humidity in assessing human discomfort in hot and humid weather conditions, found that the thermal discomfort had a synergy with the air quality in extreme weather conditions. This is consistent with our findings for GC, Egypt, showing a positive correlation of PM10 and ozone with temperature. These results also agree with those of a study of Birmingham, UK, by Kalisa et al. [19], a study of Athens, Greece, by Theoharatos et al. [18], and a study of 17 French cities by Pascal et al. [21]. However, our results for ozone, which indicate a significant positive, but rather weak, correlation with temperature, do not concur with the findings of a study of three cities in the Center Region of France by Lacour et al. [32], which found ozone to strongly correlate with temperature, or the findings of Kalisa et al. [19], in which the time series of ozone exhibited the most pronounced variation, among the other air pollutants, in relation to HW.

The positive correlation between PM10 and temperature may be attributed in part to the fact that clear skies and active photochemistry during HWs facilitate the transformation of anthropogenic or natural volatile precursors into secondary fine particles, thereby increasing the PM10 concentration in air [19]. Regarding these precursors, it is most probable that the emission of volatile organic compounds (VOC) by the vegetation is enhanced when plants are subjected to an intense heat stress during the HWs [33]. Moreover, air pollution levels generally tend to increase during HWs due to low winds that prevail, leading to stagnancy of air and poor dispersion conditions, which results in the accumulation of all types of pollutants in the atmosphere. However, this stagnation, which could explain part of the PM10 increase with temperature, does not seem to be consistent with the lack of visible effect on the NO_2 concentration. This contradicts what was reported by Kalisa et al. [19], Theoharatos et al. [18], and Pearce et al. [34], namely that NO_2 correlated positively with temperature. A possible explanation for this discrepancy could be that our analysis focused mostly on summer months (June to August), when the NO_2 concentration is the lowest in Cairo and when there are complex photochemical interactions with ozone triggered by sunlight and nitrogen oxides (NOx), in which NO_2 can act as a source or a sink of O_3, depending on their availability [20].

For ozone, the "modest" increase could be explained by the fact that HWs coincide with clear summer skies, which are obviously favorable for ozone formation. This finding agrees with the results of Mostafa et al. [16], who reported that ozone concentration increased with temperature, i.e., in the summer season and the daytime, and that the highest ozone concentration levels in GC tend to appear in the summer season. However, the relationship between ozone and temperature depends on the availability of local resources (sunshine, ozone precursors, etc.) and large-scale atmospheric circulations, and it usually does not follow a simple linear positive relationship [20]. Therefore, more research is needed in this domain, specifically with more data available to allow for a deeper examination of the local and global air pollution sources.

Further, the causal relationship between HWs and air pollution, especially PM10, may also be of interest. Indeed, a previous study of the Egyptian climate (Mostafa et al. [22]) showed that HWs are synoptic phenomena that strike the whole Egyptian territory at the same time, while PM10 concentrations are much more variable (spatially); therefore, it can be argued that HWs increase the PM10 concentration, and PM10 cannot be considered as the cause of the occurrence of HWs. However, PM10 could aggravate the HWs locally.

5. Conclusions

Between 2005 and 2023, the frequency, intensity, and duration of HWs striking the GC area have increased. Although HW days could be occasionally observed as early as March or as late as October, the most severe events, i.e., those lasting at least 5 days, occurred from June to August. In these summer months, the air pollutants (PM10, NO_2, and O_3) are essentially produced locally because the advection of mineral dust from the deserts surrounding the city or the biomass burning plumes from the Nile Delta mostly occur in spring and autumn, respectively [35]. The examination of the time series of temperature and air pollutants concentrations, and the quantification of their correlation yielded contrasted results:

1. Temperature and PM10 are strongly and positively correlated (R^2 = 0.84). On average, PM10 is around 60 $\mu g/m^3$ when the daily maximum temperature is between 27 and 30 °C, but this concentration doubles when the temperature increases above 40 °C during the HWs.
2. Ozone concentration is also positively correlated with temperature, but less strongly (R^2 = 0.24) than PM10. On average, its concentration increases by 10% (between 50 and 60 $\mu g/m^3$) when the temperature increases from 30 to 40 °C.
3. Conversely, there is no detectable impact (R^2 = 0.001) of temperature on the NO_2 concentration.

Generally, low winds prevail during HWs, which favors the accumulation of air pollutants and could explain, in part, the higher levels of PM10 during HWs. However, the NO_2 and ozone concentrations do not increase as do those of PM10. Therefore, the strong positive correlation between PM10 and temperature may rather be attributed to the more active photochemistry which accompanies the HW conditions, favors the formation of secondary aerosols, and generates higher concentrations of PM10 in the air. Moreover, under heat stress, the vegetation probably emits more VOCs to foster this conversion. However, more research is clearly necessary to identify and apportion the real reasons for the PM10 increase during HWs.

A possible explanation of the unexpected non-significant correlation of NO_2 with temperature can be the timing of the study (mostly summer), taking into consideration that NO_2 concentrations tend to decrease in the summer season. Regarding ozone, the significant positive correlation between its concentration and temperature could be easily explained by a more active generation under the clear sky condition of HWs, but the fact that the effect of these HWs is not as marked as that in other cities still requires clarification. Local ozone sources and atmospheric circulations must be further analyzed in order to explain the "modest" increase in ozone observed in GC during HWs.

Our evaluation of the role of the three pollutants shows that PM10 played the greatest role in altering the AQHI during the HWs, shifting the health risk from "moderate" to "high".

These findings are a matter of concern because the frequency of severe HWs is expected to continue increasing in the future as a result of global warming of the earth's climate. This also emphasizes the need for more research on the correlation between HWs and air pollution, specifically in examining the concurrent HWs and increasing air pollution episodes. The results of such research would help in the establishment of public health early warning systems.

Author Contributions: Conceptualization, M.M.A.W.; methodology, A.N.M., M.M.A.W. and S.C.A.; resources and validation, A.S.Z.; formal analysis and visualization, A.N.M. and S.C.A.; writing—original draft preparation, A.N.M.; writing—review and editing, S.C.A.; supervision, M.M.A.W. and S.M.R. All authors have read and agreed to the published version of the manuscript.

Funding: This research received no external funding.

Institutional Review Board Statement: Not applicable.

Informed Consent Statement: Not applicable.

Data Availability Statement: The data presented in this study are not publicly available due to their ownership by the government. Access to these datasets necessitates a formal request.

Acknowledgments: The authors wish to thank the Egyptian Meteorological Authority (EMA) and the Egyptian Environmental Affairs Agency (EEAA) for providing the data used in the study.

Conflicts of Interest: The authors declare no conflicts of interest.

References

1. Aboelkhair, H.; Morsy, M. Extreme Warm and Cold Waves Derived from Multiple High-Resolution Gridded Datasets in Egypt. *Theor. Appl. Clim. Climatol.* **2023**, *155*, 1321–1341. [CrossRef]
2. AirNow AirNow Department of State. Available online: https://www.airnow.gov/international/us-embassies-and-consulates/#Egypt$Cairo (accessed on 14 November 2023).
3. AMS Heat Wave—Glossary of Meteorology. Available online: https://glossary.ametsoc.org/wiki/Heat_wave (accessed on 30 December 2023).
4. Boraiy, M.; El-Metwally, M.; Wheida, A.; El-Nazer, M.; Hassan, S.K.; El-Sanabary, F.F.; Alfaro, S.C.; Abdelwahab, M.; Borbon, A. Statistical Analysis of the Variability of Reactive Trace Gases (SO_2, NO_2 and Ozone) in Greater Cairo during Dust Storm Events. *J. Atmos. Chem.* **2023**, *80*, 227–250. [CrossRef]
5. Ceccherini, G.; Russo, S.; Ameztoy, I.; Francesco Marchese, A.; Carmona-Moreno, C. Heat Waves in Africa 1981-2015, Observations and Reanalysis. *Nat. Hazards Earth Syst. Sci.* **2017**, *17*, 115–125. [CrossRef]
6. El-Metwally, M.; Alfaro, S.C.; Abdel Wahab, M.; Chatenet, B. Aerosol Characteristics over Urban Cairo: Seasonal Variations as Retrieved from Sun Photometer Measurements. *J. Geophys. Res. Atmos.* **2008**, *113*, 0148–0227. [CrossRef]
7. Frich, P.; Alexander, L.V.; Della-Marta, P.; Gleason, B.; Haylock, M.; Tank Klein, A.M.G.; Peterson, T. Observed Coherent Changes in Climatic Extremes during the Second Half of the Twentieth Century. *Clim. Res.* **2002**, *19*, 193–212. [CrossRef]
8. Janyasuthiwong, S.; Choomanee, P.; Bualert, S.; Maneejantra, S.; Charoenpun, T.; Chommon, W.; Jitjun, S. Biogenic Volatile Organic Compound Emission from Tropical Plants in Relation to Temperature Changes. *Environ. Chall.* **2022**, *9*, 100643. [CrossRef]
9. Kalisa, E.; Fadlallah, S.; Amani, M.; Nahayo, L.; Habiyaremye, G. Temperature and Air Pollution Relationship during Heatwaves in Birmingham, UK. *Sustain. Cities Soc.* **2018**, *43*, 111–120. [CrossRef]
10. Katzan, J.; Owsianowski, S. *A Qualitative Vulnerability and Adaptation Assessment among Pregnant Women and Mothers of Children under Five Protecting Health from Heat Stress in Informal Settlements of the Greater Cairo Region*; Deutsche Gesellschaft für Internationale Zusammenarbeit (GIZ) GmbH: Bonn, Germany, 2017.
11. Khomsi, K.; Chelhaoui, Y.; Alilou, S.; Souri, R.; Najmi, H.; Souhaili, Z. Concurrent Heat Waves and Extreme Ozone (O3) Episodes: Combined Atmospheric Patterns and Impact on Human Health. *Int. J. Environ. Res. Public. Health* **2022**, *19*, 2770. [CrossRef] [PubMed]
12. Klingelhöfer, D.; Braun, M.; Brüggmann, D.; Groneberg, D.A. Heatwaves: Does Global Research Reflect the Growing Threat in the Light of Climate Change? *Glob. Health* **2023**, *19*, 56. [CrossRef]
13. Lacour, S.A.; De Monte, M.; Diot, P.; Brocca, J.; Veron, N.; Colin, P.; Leblond, V. Relationship between Ozone and Temperature during the 2003 Heat Wave in France: Consequences for Health Data Analysis. *BMC Public Health* **2006**, *6*, 261. [CrossRef]
14. Masoud, A.A. Spatio-Temporal Patterns and Trends of the Air Pollution Integrating MERRA-2 and in Situ Air Quality Data over Egypt (2013–2021). *Air Qual. Atmos. Health* **2023**, *16*, 1543–1570. [CrossRef] [PubMed]
15. Metaxas, D.A.; Kallos, G. Heat Waves from a Synoptic Point of View. *Riv. Meteorol. Aeronaut.* **1980**, *2*, 107–119.
16. Mohamed, M.A.E.H.; Hwehy, M.M.A.; Moursy, F.I.; El-Tantawi, A.M. The Synergy of Ambient Air Quality and Thermal Discomfort: A Case Study of Greater Cairo, Egypt. *J. Agrometeorol.* **2023**, *25*, 553–559. [CrossRef]
17. Morsy, M.; El Afandi, G. Decadal Changes of Heatwave Aspects and Heat Index over Egypt. *Theor. Appl. Climatol.* **2021**, *146*, 71–90. [CrossRef]
18. Mostafa, A.N.; Wheida, A.; El Nazer, M.; Adel, M.; El Leithy, L.; Siour, G.; Coman, A.; Borbon, A.; Magdy, A.W.; Omar, M.; et al. Past (1950–2017) and Future (−2100) Temperature and Precipitation Trends in Egypt. *Weather. Clim. Extrem.* **2019**, *26*, 100225. [CrossRef]
19. Mostafa, A.N.; Zakey, A.S.; Alfaro, S.C.; Wheida, A.A.; Monem, S.A.; Abdul Wahab, M.M. Validation of RegCM-CHEM4 Model by Comparison with Surface Measurements in the Greater Cairo (Egypt) Megacity. *Environ. Sci. Pollut. Res.* **2019**, *26*, 23524–23541. [CrossRef] [PubMed]
20. Mostafa, A.N.; Zakey, A.S.; Monem, A.S.; Abdel Wahab, M.M. Analysis of the Surface Air Quality Measurements in The Greater Cairo (Egypt) Metropolitan. *Glob. J. Adv. Res.* **2018**, *5*, 207–214.
21. National Weather Service During a Heat Wave. Available online: https://www.weather.gov/safety/heat-during#:~:text=Use%20air%20conditioners%20or%20spend,hotter%20than%2090%C2%B0F (accessed on 30 December 2023).
22. Papanastasiou, D.K.; Melas, D.; Kambezidis, H.D. Heat Waves Characteristics and Their Relation to Air Quality in Athens. *Glob. Nest J.* **2014**, *16*, 919–928.
23. Pascal, M.; Wagner, V.; Alari, A.; Corso, M.; Le Tertre, A. Extreme Heat and Acute Air Pollution Episodes: A Need for Joint Public Health Warnings? *Atmos. Environ.* **2021**, *249*, 118249. [CrossRef]

24. Pearce, J.L.; Beringer, J.; Nicholls, N.; Hyndman, R.J.; Tapper, N.J. Quantifying The Influence of Local Meteorology on Air Quality Using Generalized Additive Modeling. *Atmos. Environ.* **2011**, *45*, 1328–1336. [CrossRef]
25. Potsdam Institute for Climate Impact Research and Climate Analytics. In *Why a 4 °C Warmer World Must Be Avoided Turn Down the Heat*; Potsdam Institute for Climate Impact Research: Potsdam, Germany, 2012.
26. Robinson, P.J. On the Definition of a Heat Wave. *J. Appl. Meteorol.* **2001**, *40*, 762–775. [CrossRef]
27. Said, S.; Salah, Z.; Wahab, M.M.A.; Alfaro, S.C. Retrieving PM10 Surface Concentration from AERONET Aerosol Optical Depth: The Cairo and Delhi Megacities Case Studies. *J. Indian. Soc. Remote Sens.* **2023**, *51*, 1797–1807. [CrossRef]
28. Saleh, S.M.; Heggi, M.A.M.; Abdrabbo, M.A.A.; Farag, A.A. Heat waves investigation during last decades insome climatic regions in egypt. *Egypt. J. Agric. Res.* **2017**, *95*, 863–889. [CrossRef]
29. Stieb, D.M.; Burnett, R.T.; Smith-Doiron, M.; Brion, O.; Hwashin, H.S.; Economou, V. A New Multipollutant, No-Threshold Air Quality Health Index Based on Short-Term Associations Observed in Daily Time-Series Analyses. *J. Air Waste Manag. Assoc.* **2008**, *58*, 435–450. [CrossRef] [PubMed]
30. Theoharatos, G.; Pantavou, K.; Mavrakis, A.; Spanou, A.; Katavoutas, G.; Efstathiou, P.; Mpekas, P.; Asimakopoulos, D. Heat Waves Observed in 2007 in Athens, Greece: Synoptic Conditions, Bioclimatological Assessment, Air Quality Levels and Health Effects. *Environ. Res.* **2010**, *110*, 152–161. [CrossRef]
31. UK Met Office What Is a Heatwave? Available online: https://www.metoffice.gov.uk/weather/learn-about/weather/types-of-weather/temperature/heatwave (accessed on 30 December 2023).
32. Wheida, A.; Nasser, A.; El Nazer, M.; Borbon, A.; Abo El Ata, G.A.; Abdel Wahab, M.; Alfaro, S.C. Tackling the Mortality from Long-Term Exposure to Outdoor Air Pollution in Megacities: Lessons from the Greater Cairo Case Study. *Env. Environ. Res.* **2018**, *160*, 223–231. [CrossRef]
33. WHO Heat and Health. Available online: https://www.who.int/news-room/fact-sheets/detail/climate-change-heat-and-health (accessed on 30 December 2023).
34. WMO Extreme Weather. Available online: https://wmo.int/topics/extreme-weather (accessed on 30 December 2023).
35. WMO Heatwave. Available online: https://wmo.int/topics/heatwave#:~:text=A%20heatwave%20can%20be%20defined,power%20shortages%20and%20agricultural%20losses. (accessed on 30 December 2023).